

**Biomechanics of a Bifurcating Green Plant, Part 1:****ABSTRACT**

Analytic study of the xylem flow in a bifurcating green plant is presented. The model involves a set of non-linear differential equations, which are tackled using the perturbation method of solutions. Solutions of the velocity, temperature, concentration, Nusselt and Sherwood numbers are obtained and presented graphically. It is observed that increase in the bifurcation angle increases the flow velocity and concentration, Nusselt and Sherwood numbers, whereas the soil parameter (magnetic field force) decreases the velocity and Nusselt number but increases the concentration and Sherwood number. These results have tremendous effect on the growth and yield of the plant. In particular, the increase in the transport velocity and concentration tend to increase the rate at which water and nutrients are made available to the plant, thus enhancing the growth and yield of the plant (crops); the variation in the electrolytic strength of the soil mineral salt water leading to a lower or higher Lorentz force tends to accounts for why some plants do well in some regions than in the others. Furthermore, it is seen that when the angle of bifurcation is zero (i.e.  $\alpha = 0$ ) and the magnetic field and thermal diffusion parameter are neglected the flow structures reduce to those of [4].

**Keyword:** *biomechanics, bifurcation, green plants, magnetic field, soil nature, xylem flow*

**1 Introduction**

Green plants play very important roles in the lives of man, animals and their environments. They produce oxygen that enriches our environment through photosynthetic activities. They are sources of food for both man and animals, planks for construction of buildings and other structures, and raw material for the industrial production of paper. More so, green plants protect the environment from erosion.

The production of crops and animals for the benefits of man is a global objective that calls for the cooperation of all, and the services of experts, especially those in the fields of science. A good production of crops and animals depends on a number of favourable conditions. In particular, the growth and yield of crops depend on the soil factor that includes the availability of soil water and nutrients, soil temperature and soil pollution; atmospheric factor that consists of the presence of sunlight, humidity, temperature and wind; the plant factor that embraces the physical properties of the plant system; transpiration that is influenced by the soil, atmospheric and plant factors [1]. Furthermore, plants nutrients consist of about sixteen known essential elements present in the soil. They are classified into two: the macro- and micro- elements. The macro-elements comprise carbon, hydrogen, nitrogen, phosphorus, potassium, calcium, magnesium and sulphur, and are required in large quantities. The micro-elements, which include copper, zinc, molybdenum, boron, chlorine and iron are required in small quantities. The soil water, which is continually absorbed into the plants exists as alkaline and salts in the form of nitrogen, sulphur, potassium, magnesium, iron, zinc, molybdenum, manganese and boron [1]. These solutions are electrolytes; therefore exist as ions, which help to carry electricity at different degrees. The motion of these ions in presence of a magnetic field (such as the Earth magnetic field that is caused by the rotation of the Earth) results in electric currents, which subsequently gives rise to a magnetic field force (the Lorentz force) that in turn, gives the flow a new orientation [2, 3]. Taking cognizance of the afore-mentioned factors, it becomes evident that a soil may be fertile but may not be productive. This study attempts to examine the roles of the said factors in the transport of soil mineral salt water through the stem via the bifurcations to the leaves of the green plants (crops) with their attendant effects on their growth and yield.

[4] examined the dynamics of the fluid in the xylem and phloem vessels of the tree trunk whose length is far greater than the diameter (i. e.  $l \gg d$ ) such that the ratio of the length to diameter, otherwise called the aspect ratio is far less than one (i.e.  $\mathfrak{R} = d/l \ll 1$ ). According to him, the flow in this type of channel is Poiseuille, laminar and steady. Furthermore, his model found application in green plants like iroko, coconut, paw-paw, plantain and the likes. However, [4] model has some limitations. It cannot explain the flow mechanism in plants that develop branches early in their growth stage (as in desert plants, guavas, mangoes, pears, indian almond and so on). In such plants, their aspect ratio is

approximately greater than or equal to one, and in which case, the flow structure is seen to depend mostly on the angle of the bifurcation and Reynolds number. Similarly, the model did not consider the effects of bifurcation angle and the nature of the soil on the growth and yield of the plant (crop). Therefore, we are motivated to examine, amidst others, the effects of these parameters on the xylem flow situation.

Studies have shown that the fluid bearing vessels of the green plants are porous; the fluids are bio-magnetic; the flow naturally convective. Therefore, apart from a few antiquated literatures on green plants, our study of the biomechanics of green plants shall be reviewed majorly in the light of the existing reports on the hydrodynamics of fluids in channels. For example, [5, 6] gave literature overviews of the biomechanics of green plants. [4] investigated the xylem and phloem flows at low Reynolds number in a tree trunk with aspect ratio far less than one. He modeled the vessel pores as valves representing the permeability of a porous medium; solved the governing equations analytically by the method of Laplace transforms, and observed that, for the phloem flow the concentration is confined near the wall of the green plant and is negative. While for the xylem flow, the concentration is more valid at the centre and is positive. Additionally, his results show that concentration decreases as porosity increases.

The concept of bifurcation (in sense that a flow system divides into two or more daughter channels) is seen in both natural and industrial settings. Therefore, it has relevance in science and engineering. To this end, a number of literatures exist on the dynamics of fluid in such systems. For example, [7] introduced the use of theoretical approach or mathematical tools in the study of branching flows; [8] studied the effect of bifurcation angles on the steady flow in a straight terminal aneurysm model with asymmetric outflow through the branches using the Laser-Doppler velocity and fluctuating intensity distribution. They observed that the size of the recirculation zones in the afferent vessel, the flow activity inside the aneurysm, and the shear stress acting on the aneurysmal wall increase as the bifurcation angle increases. More so, [9, 10] examined numerically and experimentally the flow structure in bifurcating pipes, and observed that the increase in bifurcation angle increases the inlet pressure, which subsequently increases the flow velocity. [11] examined theoretically the behaviour of an incompressible side-branching flow at high Reynolds number, and compared their results with that of direct numerical simulation at moderate Reynolds number. They observed that near the branch the flow adjusts itself to the imposed downstream pressure in the daughter through a jump in the flow properties across the daughter entrance. Furthermore, they noticed that for large pressure drops in the daughter tube the fluid is sucked in at high velocities from the mother and thereby provides a favourable upstream feedback. [12] investigated the equilibrium configuration and stability of a channel bifurcation in braided rivers, and showed that an increase in bifurcation angle increases the transport velocity. [13] showed that changes in bifurcation angle alter the flow condition and changes the magnitude of the wall shear stress. [14] investigated a three-dimensional one-to-two symmetrical flow in which the mother is straight and of circular cross-section, containing a fully developed incident motion, while the diverging daughters are straight and of semi-circular cross-section. Using the method of direct numerical simulation and slender modeling for a variety of Reynolds number and divergent angles, they observed that a flow separation or reversal occurs at the corners of the junction, and the inlet pressure increases as the bifurcation angle increases. [15] studied blood flow in bifurcating arteries using the method of regular perturbation, and noticed that an increase in bifurcation angle and Reynolds number increase the transport velocity factor.

The flow through porous media is prevalent in both natural and artificial settings. Therefore, it is of great interest in science and engineering. For this cause, [16] investigated the flow in a rotating straight pipe and showed that the Nusselt number increases with increase in porosity. Furthermore, [17] studied the flow in a curved porous channel with rectangular cross-section filled with a fluid saturated porous medium with the flow driven by a constant azimuthally pressure gradient used the generalized Fourier series method of solution, and found that the velocity profiles depend on the geometry of the channel and Darcy number. [18] examined the fluid-mechanical aspect of the flow in bifurcating arteries, and observed that an increase in bifurcation angle and Reynolds number produces a commensurate increase in the wall shear stress. Similarly, the flow problems through non-porous channels in the presence of chemical reactions were also considered. [19] studied a two-dimensional flow of an incompressible viscous fluid through a non-porous channel with heat generation and chemical reaction by the methods of similarity transformation, homotopy analysis and numerical. They observed that an increase in the Reynolds number decreases the tangential velocity but increases the heat and mass transfer; the increase in the Eckert number and heat generation/absorption parameter increase the temperature; the increase in the chemical reaction

parameter decreases the concentration profiles, and an increase in the Grashof number increases the flow velocity.

The study of the flow of fluids has been extended to include the effect of magnetic field. [20] considered the flow of viscous incompressible fluid embedded with small spherical particles in a non-conducting channel with hexagonal cross-section in the presence of a transverse magnetic field using the method of integral transformation, noticed that the velocity of the fluid and particles decrease with increase in the intensity of magnetic field. [21] investigated the effect of magnetic field on the flow in a rectangular enclosure using perturbation technique, reported that the imposed magnetic field diminished the wall shear stress. [22] examined the influence of magnetic field on the skin friction factor of a steady fully developed laminar flow through a pipe by experimental and finite difference numerical scheme. They observed that the pressure drop varies in proportion to the square of the magnetic field and the sine angle; the pressure is proportional to the flow rate, and the axial velocity asymptotically approaches its limit as the Hartmann number becomes large.

More so, there are research reports on the magneto-hydrodynamic convective flow. Magneto-hydrodynamic convective heat and mass transfer in porous and non-porous media is of considerable interest in technical field due to its applications in industries, geothermal, high temperature plasma, liquid metal and MHD power generating systems. [23] studied the free convection flow through a vertical porous channel in the presence of an applied magnetic field using the finite difference numerical approach, and noticed that the velocity decreases with the increase in the magnetic and porosity parameters throughout the region. [24] considered the fully developed mixed convective flow in a vertical channel filled with nano-fluids in the presence of a uniform transverse magnetic field using the closed form solutions. They observed that magnetic field enhances the nano-fluid velocity in the channel; the induced magnetic field vanishes in the central region of the channel. In addition, they noticed that the critical Raleigh number at the onset of the instability of the flow is strongly dependent on the volume fraction of nano-particles and the magnetic field. [25] studied the magneto-hydrodynamic free convective and oscillatory flow through a vertical channel filled with porous medium with non-uniform wall temperatures using the method of asymptotic expansions. They noticed that the velocity of the fluid increases with the increase in Grashof number but decreases due to increase in the porosity parameter or magnetic parameter; the temperature of the fluid decrease as radiation parameter, heat generation/absorption parameter or Prandtl number increases. Furthermore, they found that the skin-friction coefficient at the wall increases with the increase in Grashof number but decreases with the increase in porosity parameter, magnetic parameter, radiation parameter, heat generation/absorption parameter or Prandtl number; the Nusselt number at the wall increases due to the increase in the radiation parameter, heat generation/absorption parameter or Prandtl number. [26] investigated the effects of magnetic field and convective force on the flow in bifurcating porous fine capillaries, and found that magnetic field reduces the flow velocity, whereas the convective force increases it. More so, [27] examined analytically the blood flow in bifurcating arteries, and observed that an increase in heat exchange parameter and Grashof number increase the velocity, concentration and Nusselt number of the flow while an increase in the heat exchange parameter increases the Sherwood number. [28] considered analytically a span-wise fluctuating magneto-hydrodynamic (MHD) convective flow problem of a viscous, incompressible and electrically conducting fluid through a porous medium filled in an infinite vertical channel, with the walls subjected to span-wise cosinusoidally varying species concentration and temperature. They observed that the velocity increases with the increase in the buoyancy forces due to concentration and thermal diffusions, and permeability but decreases with the increase in the magnetic field, Prandtl number, heat generation/absorption parameter, Schmidt number, radiation parameter and frequency of oscillations; the skin-friction amplitude increases with the increase in the Grashof number (due to concentration gradient), permeability, Schmidt number and radiation parameter while it decreases with the increase in the Grashof number, magnetic field, Prandtl number and heat generation/absorption. Also, they noticed that there is always a phase lead in the skin-friction, which increases with the increase in Grashof number (due to concentration gradient), permeability and radiation parameter but decreases with the increase in magnetic field, Prandtl number, heat generation/absorption, and Schmidt number; the temperature decreases as Prandtl number, heat generation/absorption and frequency of oscillations increase; the species concentration also decreases with the increase in Schmidt, radiation parameter and frequency of oscillations. Furthermore, they saw that the amplitudes of the Nusselt number and Sherwood number increase sharply and decrease mildly with the increase in the different parameters involved; there is always a phase lag for the Sherwood number. [29] considered the flow in a bifurcating river, and found that

bifurcation angle, Reynolds number and thermal differentials increase the velocity factor, while the Hartmann number decreases it. [30] elaborately investigated analytically the effects of radiation and hall current on the MHD free convective three -dimensional flow of an incompressible viscous fluid in a vertical parallel plates channel filled with a porous medium. They observed that the velocity component for the primary flow enhances with the increase in Reynolds number, Darcy parameter, hall parameter, Grashof number, Peclet number and pressure gradient but reduces with the increase in the intensity in magnetic field (Hartmann number) and radiation parameter; the velocity component for secondary flow enhances with the increase in Darcy number and hall parameter but reduces with the increase in Reynolds number, magnetic field, Gashof number, Peclet number, pressure gradient and radiation parameter; the resultant velocity enhances with the increase in Reynolds number, Darcy number, hall parameter and pressure gradient but reduces with the increase in magnetic field, Grashof number, Peclet number, radiation parameter and frequency of oscillation. Similarly, they noticed that the temperature reduces with increase in radiation parameter or Peclet number while it enhances initially and then gradually reduces with the increase in the frequency of oscillation; the amplitude of rate of heat transfer decreases with the increase in radiation parameter and Peclet number; the phase angle decreases with the increase in the Peclet number but increases with increase in the radiation parameter; there is a phase log for the values of the frequency of oscillations. Furthermore, they saw that the amplitude increases with the increase in Reynolds number, pressure gradient, Grashof number and hall parameter, permeability of the porous medium, Peclet number, radiation parameter for small values of frequency of oscillation but decreases for large values of frequency of oscillation; the effect of Darcy number is insignificant for large values of frequency of oscillations. More so, it is seen that the amplitude decreases with increase in magnetic field; the phase angle increases with increase in Reynolds number, hall parameter, Peclet number, radiation parameter and Grashof number but decreases with the increase in Darcy number, magnetic field and pressure gradient.

The purpose of this paper, which is the part one of this study, is to investigate the effects of bifurcation angle and the nature of the soil in which the plant grows on the flow of mineral salt water in a green plant that bifurcates with their attendant implications on agricultural productivity.

The paper is organized as follows: the material and methods, results, discussion and conclusion.

## 2 Methodology

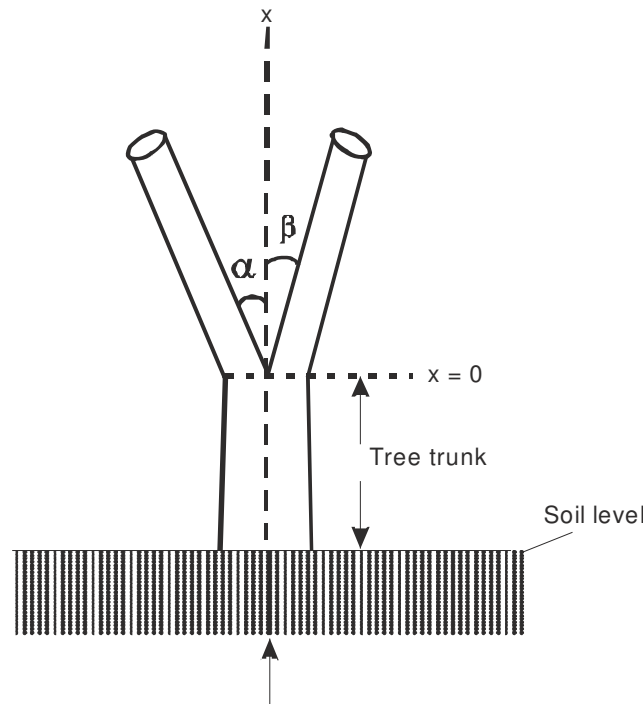


Fig. 1 The physical representation of the model

In a typical green plant, the carriers of the fluids are the xylem and phloem vessels. The phloem vessels carry the manufactured materials from the leaves down through the stem to other parts of the tree. Here, the flow is in the direction of gravity. For the xylem flow, which is anti-gravity, the soil mineral salt water is absorbed by the roots, and is conveyed through the stem (tree trunk) to the leaves. A close examination of the cross-section of a typical green plant shows that it is made up of interconnected spores and capillaries through which the fluids flow. Therefore, the plant tissues are porous. The mineral salt water, by the nature of its chemical content is electrolytic, and therefore, is magnetically susceptible. The fluid viscosity is a function of temperature and magnetic field. We shall also assume that the bifurcating channels are symmetrical; the flow is creppy, with a Reynolds number of about 0.02 [4]. If therefore,  $(u', v', w')$  are the velocity vectors with respect to the orthogonal coordinate directions  $(r', \theta', x')$ ,  $\rho$  the fluid density,  $p'$  the pressure,  $\mu$  the viscosity,  $\mu_m$  the magnetic permeability of the fluid,  $\mathbf{g}$  the gravitational field vector acting in the reverse direction of the flow,  $T'$  and  $C'$  are, respectively, the fluid temperature and concentration (quantity of material being transported), while  $T_w$  and  $C_w$  are the constant wall temperature and concentration at which the channel is maintained, whereas  $T_\infty$  and  $C_\infty$  are, respectively, the temperature and concentration at equilibrium. More so, assuming that the flow is fully developed in the mother channel and the velocity is symmetrical about the  $\theta'$  axis such that variations about  $\theta'$  is zero the coordinate becomes  $(r', x')$  and the velocity vector becomes  $(u', w')$ , then the models describing the motion of the fluid in the bifurcating green plant in cylindrical polar coordinates as shown in Fig 1, considering Boussinesq approximation are:

$$\frac{1}{r'} \frac{\partial(r'u')}{\partial r'} + \frac{\partial u'}{\partial x'} = 0 \quad (1)$$

$$0 = -\frac{\partial p'}{\partial r'} + \mu \left( \frac{\partial^2 u'}{\partial r'^2} + \frac{1}{r'} \frac{\partial u'}{\partial r'} - \frac{u'}{r'^2} + \frac{\partial^2 u'}{\partial x'^2} \right) \quad (2)$$

$$0 = -\frac{\partial p'}{\partial x'} + \mu \left( \frac{\partial^2 w'}{\partial r'^2} + \frac{1}{r'} \frac{\partial w'}{\partial r'} + \frac{\partial^2 w'}{\partial x'^2} \right) + \rho' g \beta_t (T' - T_\infty) + \rho' g \beta_c (C' - C_\infty) - \frac{\mu v'}{\kappa} - \frac{\sigma_e B_o^2 w'}{\rho'^2 \mu_m} \quad (3)$$

$$\rho C_p \left( u' \frac{\partial T'}{\partial x'} + v' \frac{\partial T'}{\partial r'} \right) = k_o \left( \frac{\partial^2 T'}{\partial r'^2} + \frac{1}{r'} \frac{\partial T'}{\partial r'} + \frac{\partial^2 T'}{\partial x'^2} \right) - Q(T' - T_\infty) \quad (4)$$

$$u' \frac{\partial C'}{\partial x'} + v' \frac{\partial C'}{\partial r'} = D \left( \frac{\partial^2 C'}{\partial r'^2} + \frac{1}{r'} \frac{\partial C'}{\partial r'} + \frac{\partial^2 C'}{\partial x'^2} \right) + k_r^2 (C' - C_\infty) \quad (5)$$

The general analysis of the physical geometry of the problem presented in Fig.1 shows that the boundary conditions can be split into two distinct parts, namely, mother or upstream,  $x < 0$  and daughter or downstream,  $x > 0$ .

For the upstream,

$$(u', w') = (1, 1) \text{ and } (T', C') = (T_\infty, C_\infty) \quad \text{at } r' = 0 \quad (6)$$

$$(u', w') = (0, 0) \text{ and } (T', C') = (T_w, C_w), \quad \text{at } r' = 1 \quad (7)$$

and  
for the downstream,

$$(u', w') = (0, 0) \text{ and } (T', C') = (0, 0) \text{ at } r' = 0 \quad (8)$$

$$(u', w') = (0, 0) \text{ and } (T', C') = (\gamma_1 T_w, \gamma_2 C_w), \gamma_1 = \gamma_2 < 1 \text{ at } r' = \alpha x' \quad (9)$$

Introducing the following non-dimensional parameters

$$r = \frac{r'}{R_o}, x = \frac{\Re x'}{l}, w = \frac{w' R_o}{\nu}, \Theta = \frac{T' - T_\infty}{T_w - T_\infty}, \Phi = \frac{C' - C_\infty}{C_w - C_\infty},$$

$$p = \frac{(p' - p_\infty) r_o^3}{\rho \nu}, \text{Re} = \nu l, M^2 = \frac{\sigma_e B_o^2}{\rho \mu \mu_m}, N^2 = \frac{Q}{k_o}, \chi^2 = \frac{R_o}{\kappa}, \delta_1^2 = \frac{k_r^2}{D},$$

$$Sc = \frac{\nu}{D}, \text{Pr} = \frac{\mu C_p}{k_o}, Gr = \frac{g \beta_1 (T_w - T_\infty)}{\nu^2}, Gc = \frac{g \beta_2 (C_w - C_\infty)}{\nu^2}$$

$$Pe_m = \text{Re} Sc, Pe_h = \text{Re} \text{Pr}, M_1^2 = \chi^2 + M^2,$$

where  $\beta_1$  and  $\beta_2$  are the volumetric expansion coefficient for temperature and concentration respectively,  $\Theta$  and  $\Phi$  are the non-dimensionalized temperature and concentration, respectively,  $\kappa$  is the permeability parameter of the porous medium,  $B_o$  is the applied uniform magnetic field strength due the nature of the soil and the earth field,  $\sigma_e$  is the electrical conductivity of the fluid,  $k_o$  the thermal conductivity,  $C_p$  the specific heat capacity at constant pressure,  $Q$  is the heat absorption coefficient,  $D$  the diffusion coefficient,  $k_r^2$  is the rate of chemical reaction of the soil mineral salt solution,  $\alpha$  and  $\beta$  are the angles at which the plant bifurcates,  $\Re$  is the aspect ratio,  $\nu$  is the kinematic viscosity,  $R_o$  is the characteristic radius of the tree trunk,  $M^2$  is the soil parameter,  $\text{Re}$  is the Reynolds number,  $N^2$  is the environmental temperature differential parameter,  $\chi^2$  is the porosity parameter,  $\delta_1^2$  is the chemical reaction parameter,  $Sc$  the Schmidt number,  $\text{Pr}$  the Prandtl number,  $(Gr, Gc)$  are the Grashof number due to temperature and concentration differences, while  $(Pe_h, Pe_m)$  are the Peclet number due to heat and mass transfers, into (1)-(5), we have

$$\frac{1}{r} \frac{\partial(ru)}{\partial r} + \frac{\Re \partial w}{\partial x} = 0 \quad (10)$$

$$\frac{\partial^2 u}{\partial r^2} + \frac{1}{r} \frac{\partial u}{\partial r} - \frac{u}{r^2} = \frac{\partial p}{\partial r} \quad (11)$$

$$\frac{\partial^2 w}{\partial r^2} + \frac{1}{r} \frac{\partial w}{\partial r} - (M^2 + \chi^2)w = \Re \frac{\partial p}{\partial x} - Gr\Theta - Gc\Phi \quad (12)$$

$$\frac{\partial^2 \Theta}{\partial r^2} + \frac{1}{r} \frac{\partial \Theta}{\partial r} + N^2 \Theta = Pe_h \left( u \frac{\partial \Theta}{\partial r} + \Re w \frac{\partial \Theta}{\partial x} \right) \quad (13)$$

$$\frac{\partial^2 \Phi}{\partial r^2} + \frac{1}{r} \frac{\partial \Phi}{\partial r} + \delta_1^2 \Phi = Pe_m \left( u \frac{\partial \Phi}{\partial r} + \Re w \frac{\partial \Phi}{\partial x} \right) \quad (14)$$

With boundary conditions

$$(u, w) = (1, 1) \text{ and } (\Theta, \Phi) = (1, 1) \quad \text{at } r = 0 \quad (15)$$

$$(u, w) = (0, 0) \text{ and } (\Theta, \Phi) = (\Theta_w, \Phi_w), \quad \text{at } r = 1 \quad (16)$$

for the upstream  
and

$$(u, w) = (0, 0) \text{ and } (\Theta, \Phi) = (0, 0) \quad \text{at } r = 0 \quad (17)$$

$$(u, w) = (0, 0) \text{ and } (\Theta, \Phi) = (\gamma_1 \Theta_w, \gamma_2 \Phi_w), \quad \gamma_1 = \gamma_2 < 1 \quad \text{at } r = \Re \alpha x \quad (18)$$

for the downstream

A close observation shows that the (10)-(14) non-linear and highly coupled. To embark on analytical solutions, we employ the regular method of perturbation series solution of the form

$$f(r, x) = f_0(r, x) + \xi f_1(r, x) + \xi^2 f_2(r, x) + \dots \quad (19)$$

where  $\xi = \text{Re} \ll 1$  is the perturbing parameter assumed to be extremely small. The choice of this parameter is based on the fact that in such a channel the Reynolds number is usually very small. But, as the fluid flows towards the bifurcation or the nodal point, due to the change in geometrical configuration the inertial force rises such that the Reynolds number, and consequently, the momentum are increased at their own level. Now, assuming the flow is fully developed such that

$$\frac{\partial u}{\partial r} = \frac{\partial p}{\partial r} = 0, \text{ and } f_0(r, x) = f_{00}(r) - \gamma x$$

and  $f_1(r, x) = f_{10}(r) - \gamma x$ , where  $f_1$  and  $f_1$  represents the velocity, temperature and concentration in the mother (or upstream) and daughter (or downstream) sections respectively, and

$p = \Re x - \frac{\Re x^2}{\Re}$  for the pressure ( $\Re x$  is the pressure in the mother region;  $\frac{\Re x^2}{\Re}$  is the pressure in the daughter region), (see [1]) then the equations governing the flow in these streams are:

$$\frac{\partial^2 w_{00}}{\partial r^2} + \frac{1}{r} \frac{\partial w_{00}}{\partial r} - M_1^2 w_{00} = \frac{\Re \partial p_{00}}{\partial x} - Gr \Theta_{00} - Gc \Phi_{00} \quad (20)$$

$$\frac{\partial^2 \Theta_{00}}{\partial r^2} + \frac{1}{r} \frac{\partial \Theta_{00}}{\partial r} + N^2 \Theta_{00} = -\gamma \Re Pe_h w_o \quad (21)$$

$$\frac{\partial^2 \Phi_{00}}{\partial r^2} + \frac{1}{r} \frac{\partial \Phi_{00}}{\partial r} + \delta_1^2 \Phi_{00} = -\gamma \Re Pe_m w_o \quad (22)$$

with the boundary conditions

$$w_{00} = 1, \Theta_{00} = 1, \Phi_{00} = 1 \quad \text{at } r = 0 \quad (23)$$

$$w_{00} = 0, \Theta_{00} = \Theta_w, \Phi_{00} = \Phi_w \quad \text{at } r = 1 \quad (24)$$

for the upstream, and

$$\frac{\partial^2 w_{10}}{\partial r^2} + \frac{1}{r} \frac{\partial w_{10}}{\partial r} - M_1^2 w_{10} = \Re \frac{\partial p_{10}}{\partial x} - Gr \Theta_{10} - Gc \Phi_{10} \quad (25)$$

$$\frac{\partial^2 \Theta_{10}}{\partial r^2} + \frac{1}{r} \frac{\partial \Theta_{10}}{\partial r} + N^2 \Theta_{10} = -\mathfrak{R}Pe_h (w_{00} \frac{\partial \Theta_{10}}{\partial x} + w_{10} \frac{\partial \Theta_{00}}{\partial x})$$

$$(26) \quad \frac{\partial^2 \Phi_{10}}{\partial r^2} + \frac{1}{r} \frac{\partial \Phi_{10}}{\partial r} + \delta_1^2 \Phi_{10} = -\mathfrak{R}Pe_m (w_{00} \frac{\partial \Phi_{10}}{\partial x} + w_{10} \frac{\partial \Phi_{00}}{\partial x})$$

$$(27)$$

with the boundary conditions

$$w_{10} = 0, \Theta_{10} = 0, \Phi_{10} = 0 \quad \text{at } r = 0$$

$$(28)$$

$$w_{10} = 0, \Theta_{10} = \gamma_1 \Theta_w, \Phi_{10} = \gamma_2 \Phi_w, \gamma_1 < 1, \gamma_2 < 1 \quad \text{at } r = \mathfrak{R}x$$

$$(29)$$

for the downstream.

The upward transport of fluid in green plants through the xylem vessels is enhanced by (i) the suction pressure which resulted from the osmotic pressure, and (ii) the environmental thermal gradient which culminated in the convective motion of the fluid. For some green plants such as grasses, shrubs and the like only the suction pressure is enough to carry the fluid to their terminals, whereas in others like the tall trees suction pressure in addition to the buoyancy (Gr/Gc) are required to overcome the gravitational force for the fluid to get to its height. Therefore, for the case in which the suction pressure is sufficient to transport the fluid from the base to its height, buoyancy is usually neglected such that Gr/ Gc = 0 (see [4]), and for the other situation where buoyancy is not neglected Gr/Gc  $\neq$  0.

After exhaustive algebra and applying the necessary boundary conditions, we have the following solutions:

Case 1: Gr/Gc=0

For the upstream,

$$w_o(r) = \frac{\mathfrak{R}K}{M^2} \left[ \frac{I_o(M_1 r)}{I_o(M_1)} - 1 \right]$$

(30)

In the absence of magnetic field (i.e.  $M^2 = 0$ ) the velocity expression becomes

$$w_o(r) = \frac{\mathfrak{R}K}{\chi^2} \left[ \frac{I_o(\chi r)}{I_o(\chi)} - 1 \right]$$

$$(31)$$

And, this is the velocity relation in [4].

$$\Theta_o(r) = \frac{1}{J_o(N)} \left[ 1 - \frac{\mathfrak{R}Pe_h \mathfrak{R}K}{M_1^2} \left[ -\frac{1}{I_o(M_1)} \left( \frac{N}{4} + \frac{N^3}{16} \right) + \frac{N}{4} \right] J_o(N) \right] J_o(Nr)$$

$$+ \frac{\mathfrak{R}Pe_h \mathfrak{R}K}{M_1^2} \left[ -\frac{1}{I_o(M_1)} \left( \frac{N^2 r^2}{4} + \frac{N^3 r^4}{16} \right) + \frac{N}{4} \right] J_o(Nr)$$

(32)

$$\Phi_o(r) = \frac{1}{J_o(\delta_1)} \left[ 1 - \frac{\mathfrak{R}Pe_h \mathfrak{R}K}{M_1^2} \left[ -\frac{1}{I_o(M_1)} \left( \frac{\delta_1}{4} + \frac{\delta_1^3}{16} \right) + \frac{\delta_1}{4} \right] J_o(\delta_1) \right] J_o(\delta_1 r)$$

$$+ \frac{\mathfrak{R}Pe_h \mathfrak{R}K}{M_1^2} \left[ -\frac{1}{I_o(M_1)} \left( \frac{\delta_1^2 r^2}{4} + \frac{\delta_1^3 r^4}{16} \right) + \frac{\delta_1}{4} \right] J_o(\delta_1 r)$$

$$(33)$$

The Nusselt (Nu) and Sherwood(Sh) numbers are:



$$\begin{aligned}
 Nu &= \left. \frac{-\partial\Theta_o}{dr} \right|_{r=1} \\
 &= \frac{N}{J_o(N)} \left[ 1 - \frac{\gamma \Re Pe_h \Re K}{M_1^2} \left[ -\frac{1}{I_o(M_1)} \left( \frac{N}{4} + \frac{N^3}{16} \right) + \frac{N}{4} \right] J_o(N) \right] J_1(N) \\
 &\quad + \frac{\gamma \Re Pe_h \Re KN}{M_1^2} \left[ -\frac{1}{I_o(M_1)} \left( \frac{N^2}{4} + \frac{N^3}{16} \right) + \frac{N}{4} \right] J_1(N) \\
 &\quad - \frac{\gamma \Re Pe_h \Re KN}{M_1^2} \left[ -\frac{1}{I_o(M_1)} \left( \frac{N^2}{2} + \frac{N^3}{4} \right) \right] J_o(N)
 \end{aligned}
 \tag{34}$$

$$\begin{aligned}
 Sh &= \left. \frac{-\partial\Phi_o}{\partial r} \right|_{r=1} \\
 &= \frac{\delta_1}{J_o(\delta_1)} \left[ 1 - \frac{\gamma \Re Pe_h \Re K}{M_1^2} \left[ -\frac{1}{I_o(M_1)} \left( \frac{\delta_1}{4} + \frac{\delta_1^3}{16} \right) + \frac{\delta_1}{4} \right] J_o(\delta_1) \right] J_1(\delta_1) \\
 &\quad + \frac{\gamma \Re Pe_h \Re K \delta_1}{M_1^2} \left[ -\frac{1}{I_o(M_1)} \left( \frac{\delta_1^2}{4} + \frac{\delta_1^3}{16} \right) + \frac{\delta_1}{4} \right] J_1(\delta_1) \\
 &\quad - \frac{\gamma \Re Pe_h \Re \delta_1}{M_1^2} \left[ -\frac{1}{I_o(M_1)} \left( \frac{\delta_1^2}{2} + \frac{\delta_1^3}{4} \right) \right] J_o(\delta_1)
 \end{aligned}
 \tag{35}$$

Also, for the downstream,

$$w_1 = \frac{\Re K_{1,x}}{M_1^2} \left[ \frac{I_o(M_1 r)}{I_o(M_1 \Re \alpha x)} - 1 \right]
 \tag{36}$$

$$\begin{aligned}
 \Theta_1(r) &= \frac{1}{J_o(N \Re \alpha x)} \left[ \gamma_1 \Theta_w - \frac{1}{4} \left\{ -\frac{\gamma \Re^2 Pe_h}{M_1^2} \left( \frac{K}{I_o(M_1)} + \frac{K_{1,x}}{I_o(M_1 \Re \alpha x)} \right) \right. \right. \\
 &\quad \left. \left. * \left( 1 + \frac{M_1^2 (\Re \alpha x)^2}{4} \right) + \gamma \Re^2 Pe_m (K + K_{1,x}) \right\} N (\Re \alpha x)^2 J_o(N \Re \alpha x) \right] J_o(Nr) \\
 &\quad + \frac{1}{4} \left\{ -\frac{\gamma \Re^2 Pe_h}{M_1^2} \left( \frac{K}{I_o(M_1)} + \frac{K_{1,x}}{I_o(M_1 \Re \alpha x)} \right) \left( 1 + \frac{M_1^2 r^2}{4} \right) \right. \\
 &\quad \left. + \gamma \Re^2 Pe_m (K + K_{1,x}) \right\} Nr^2 J_o(Nr)
 \end{aligned}
 \tag{37}$$

$$\Phi_1(r) = \frac{1}{J_o(\delta_1 \Re \alpha x)} \left[ \gamma_1 \Theta_w - \frac{1}{4} \left\{ -\frac{\gamma \Re^2 Pe_m}{M_1^2} \left( \frac{K}{I_o(M_1)} + \frac{K_{1,x}}{I_o(M_1 \Re \alpha x)} \right) \right. \right.$$

$$\begin{aligned}
 & * \left( 1 + \frac{M_1^2 (\Re \alpha x)^2}{4} \right) + \mathcal{P} \Re^2 Pe_m (K + K_1 x) \} N(\Re \alpha x)^2 J_o(\delta_1 \Re \alpha x) J_o(\delta_1 r) \\
 & + \frac{1}{4} \left\{ - \frac{\mathcal{P} \Re^2 Pe_m \left( \frac{K}{I_o(M_1)} + \frac{K_1 x}{I_o(M_1 \Re \alpha x)} \right) \left( 1 + \frac{M_1^2 r^2}{4} \right)}{M_1^2} \right. \\
 & \left. + \mathcal{P} \Re^2 Pe_m (K + K_1 x) \right\} \delta_1 r^2 J_o(\delta_1 r)
 \end{aligned}$$

(38)

$$\begin{aligned}
 Nu &= \left. \frac{-\partial \Theta_1}{dr} \right|_{r=\Re \alpha x} \\
 &= - \left[ \frac{1}{J_o(N \Re \alpha x)} \left[ \gamma_1 \Theta_w - \frac{1}{4} \left\{ - \frac{\mathcal{P} \Re^2 Pe_h \left( \frac{K}{I_o(M_1)} + \frac{K_1 x}{I_o(M_1 \Re \alpha x)} \right)}{M_1^2} \right. \right. \right. \\
 & * \left. \left. \left( 1 + \frac{M_1^2 (\Re \alpha x)^2}{4} \right) + \mathcal{P} \Re^2 Pe_h (K + K_1 x) \right\} N^2 (\Re \alpha x)^2 J_o(N \Re \alpha x) J_1(Nr) \right. \\
 & \left. + \frac{1}{4} \left\{ - \frac{\mathcal{P} \Re^2 Pe_h \left( \frac{K}{I_o(M_1)} + \frac{K_1 x}{I_o(M_1 \Re \alpha x)} \right) \left( 1 + \frac{M_1^2 r^2}{4} \right)}{M_1^2} \right. \right. \\
 & \left. \left. + \mathcal{P} \Re^2 Pe_h (K + K_1 x) \right\} * \left[ -N^2 r^2 J_1(Nr) + 2Nr J_o(Nr) \right] \right. \\
 & \left. + \frac{1}{8} \left\{ - \mathcal{P} \Re^2 Pe_h \left( \frac{K}{I_o(M_1)} + \frac{K_1 x}{I_o(M_1 \Re \alpha x)} \right) Nr^2 J_o(Nr) \right\} \right] \\
 & \hspace{10em} (39)
 \end{aligned}$$

$$\begin{aligned}
 Sh &= \left. \frac{-\partial \Phi_1}{\partial r} \right|_{r=\Re \alpha x} \\
 &= - \left[ \frac{1}{J_o(\delta_1 \Re \alpha x)} \left[ \gamma_2 \Phi_w - \frac{1}{4} \left\{ - \frac{\mathcal{P} \Re^2 Pe_h \left( \frac{K}{I_o(M_1)} + \frac{K_1 x}{I_o(M_1 \Re \alpha x)} \right)}{M_1^2} \right. \right. \right. \\
 & * \left. \left. \left( 1 + \frac{M_1^2 (\Re \alpha x)^2}{4} \right) + \mathcal{P} \Re^2 Pe_h (K + K_1 x) \right\} \delta_1^2 (\Re \alpha x)^2 J_o(\delta_1 \Re \alpha x) J_1(\delta_1 r) \right. \\
 & \left. + \frac{1}{4} \left\{ - \frac{\mathcal{P} \Re^2 Pe_h \left( \frac{K}{I_o(M_1)} + \frac{K_1 x}{I_o(M_1 \Re \alpha x)} \right) \left( 1 + \frac{M_1^2 r^2}{4} \right)}{M_1^2} \right. \right. \\
 & \left. \left. + \mathcal{P} \Re^2 Pe_h (K + K_1 x) \right\} * \left[ -\delta_1^2 r^2 J_1(\delta_1 r) + 2\delta_1 r J_o(\delta_1 r) \right] \right. \\
 & \left. + \frac{1}{8} \left\{ - \mathcal{P} \Re^2 Pe_h \left( \frac{K}{I_o(M_1)} + \frac{K_1 x}{I_o(M_1 \Re \alpha x)} \right) \right\} \delta_1 r^2 J_o(\delta_1 r) \right]
 \end{aligned}$$

(40)

where,  $K$  = is the constant pressure gradient in the axial  $x$ -direction,  $I_n(z)$  is the modified Bessel function of order  $n$  with argument  $z$ , while  $J_n(z)$  is the ordinary Bessel function of order  $n$ .

Case 2:  $Gr/Gc \neq 0$   
For the upstream,

$$w_{00}(r) = P_* I_o(M_1 r) - \frac{1}{M_1^2} \left[ \Re K - Gr \left( L_* I_o(\sigma_+^{1/2} r) - \frac{K_v(r)}{\sigma_+} J_o(\sigma_-^{1/2} r) \right) - Gc \left( N_* I_o(\beta_+^{1/2} r) - \frac{K_w(r)}{\beta_+} J_o(\beta_-^{1/2} r) \right) \right] \quad (41)$$

$$\Theta_{00}(r) = L_* I_o(\sigma_+^{1/2} r) - \frac{K_v(r)}{\sigma_+} J_o(\sigma_-^{1/2} r) \quad (42)$$

$$\Phi_{00}(r) = N_* I_o(\beta_+^{1/2} r) - \frac{K_w(r)}{\sigma_+} J_o(\beta_-^{1/2} r) \quad (43)$$

The flow Nusselt (Nu) and Sherwood (Sh) numbers are given as:

$$Nu = - \left[ \sigma_+^{1/2} L_* I_1(\sigma_+^{1/2}) + \frac{\sigma_-^{1/2}}{\sigma_+} K_v(1) J_1(\sigma_-^{1/2}) - \frac{K_v'(1)}{\sigma_+} J_o(\sigma_-^{1/2}) \right] \quad (44)$$

$$Sh = - \left[ \beta_+^{1/2} N_* I_1(\beta_+^{1/2}) + \frac{\beta_-^{1/2} K_w(1) J_1(\beta_-^{1/2})}{\beta_+} - \frac{K_w'(1) J_o(\beta_-^{1/2})}{\beta_+} \right] \quad (45)$$

where

$$P_* = \frac{1}{M_1^2 I_o(M_1)} \left[ \Re K - Gr \left( L_* I_o(\sigma_+^{1/2}) - \frac{K_v(1)}{\sigma_+} J_o(\sigma_-^{1/2}) \right) - Gc \left( N_* I_o(\beta_+^{1/2}) - \frac{K_w(1)}{\beta_+} J_o(\beta_-^{1/2}) \right) \right]$$

$$K_v(r) = \frac{\sigma_-^{1/2} r^2}{2} \left\{ -\gamma \Re^2 Pe_h K + \gamma \Re \varepsilon \left( 1 + \frac{\Omega_+ r^2}{4} \right) - \frac{\gamma \Re \varepsilon}{\Omega_+} K_u(r) \left( 1 - \frac{\Omega_- r^2}{4} \right) \right\} J_o(\sigma_-^{1/2} r) \quad (46)$$

$$K_u(r) = 1 - \frac{\gamma \Re^2 \Re^2}{2} (Pe_h + Pe_m) \left( r + \frac{\Omega_- r^3}{2} \right) \quad (47)$$

$$K_w(r) = \frac{\beta_-^{1/2} r^2}{2} \left\{ -\gamma \Re^2 Pe_m + \gamma \Re \varepsilon \left( 1 + \frac{\Omega_+ r^2}{4} \right) - \frac{\gamma \Re \varepsilon}{\Omega_+} K_u(r) \left( 1 - \frac{\Omega_- r^2}{4} \right) \right\} \quad (48)$$

$$L_* = \frac{1}{I_o(\sigma_+^{1/2})} \left[ 1 + \frac{K_v(1)}{\sigma_+} J_o(\sigma_-^{1/2}) \right]$$

$$K_v(1) = \frac{\sigma_-^{1/2}}{2} \left\{ -\gamma \Re^2 Pe_h K + \gamma \Re \varepsilon \left( 1 + \frac{\Omega_+}{4} \right) - \frac{\gamma \Re \varepsilon}{\Omega_+} K_u(1) \left( 1 - \frac{\Omega_-}{4} \right) \right\} J_o(\sigma_-^{1/2})$$

$$\begin{aligned}\Omega_+ &= \frac{-(N^2 - M_1^2) + \sqrt{(N^2 - M_1^2)^2 + 4(N^2 M_1^2 + 2\gamma\Re\mathcal{E})}}{2} \\ \Omega_- &= \frac{-(N^2 - M_1^2) - \sqrt{(N^2 - M_1^2)^2 + 4(N^2 M_1^2 + 2\gamma\Re\mathcal{E})}}{2} \\ \sigma_+ &= \frac{-(N^2 - M_1^2) + \sqrt{(N^2 - M_1^2)^2 + 4N^2 M_1^2}}{2} \\ \sigma_- &= \frac{-(N^2 - M_1^2) - \sqrt{(N^2 - M_1^2)^2 + 4N^2 M_1^2}}{2} \\ \beta_+ &= \frac{-(\delta_1^2 - M_1^2) + \sqrt{(\delta_1^2 - M_1^2)^2 + 4\delta_1^2 M_1^2}}{2} \\ \beta_- &= \frac{-(\delta_1^2 - M_1^2) - \sqrt{(\delta_1^2 - M_1^2)^2 + 4\delta_1^2 M_1^2}}{2} \\ N_* &= \frac{1}{I_o(\beta_+^{1/2})} \left[ 1 + \frac{K_w(1)}{\beta_+} J_o(\beta_-^{1/2}) \right] \\ K_w(1) &= \frac{\beta_-^{1/2}}{2} \left\{ -\gamma\Re^2 P e_h K + \gamma\Re\mathcal{E} \left( 1 + \frac{\Omega_+}{4} \right) - \frac{\gamma\Re\mathcal{E}}{\Omega_+} K_u(I) \left( 1 - \frac{\Omega_-}{4} \right) \right\} J_o(\beta_-^{1/2}) \\ \mathcal{E} &= \gamma P e_h G r = \gamma P e_m G c\end{aligned}$$

And for the downstream,

$$\begin{aligned}w_{10}(r) &= T_* I_o(M_1 r) - \frac{1}{M_1^2} \left[ \Re K_{1x} - Gr Q_* I_o(\sigma_+^{1/2} r) - \frac{K_y(r)}{\sigma_+} J_o(\sigma_-^{1/2} r) \right. \\ &\quad \left. - Gc(S_* I_o(\beta_+^{1/2} r) - \frac{K_y(r)}{\beta_+} J_o(\beta_-^{1/2} r)) \right]\end{aligned}$$

$$\Theta_{10}(r) = Q_* I_o(\sigma_+^{1/2} r) - \frac{K_y(r)}{\sigma_+} J_o(\sigma_-^{1/2} r) \quad (49)$$

(50)

$$\Phi_{10}(r) = S_* I_o(\beta_+^{1/2} r) - \frac{K_y(r)}{\beta_+} J_o(\beta_-^{1/2} r)$$

(51)

$$\begin{aligned}Nu &= \left. \frac{-\partial\Theta_{10}}{\partial r} \right|_{r=\Re\alpha x} = - \left[ \sigma_+^{1/2} Q_* I_1(\sigma_+^{1/2} \Re\alpha x) + \frac{\sigma_-^{1/2}}{\sigma_+} K_y(\Re\alpha x) J_1(\sigma_-^{1/2} \Re\alpha x) \right. \\ &\quad \left. - \frac{K_y'(\Re\alpha x)}{\sigma_+} J_o(\sigma_-^{1/2} \Re\alpha x) \right]\end{aligned}$$

(52)

$$Sh = \frac{-\partial\Phi_{10}}{\partial r} \Big|_{r=\Re\alpha} = - \left[ \beta_+^{1/2} S_* I_1(\beta_+^{1/2} \Re\alpha) + \frac{\beta_-^{1/2}}{\beta_+} K_y(\Re\alpha) J_1(\beta_-^{1/2} \Re\alpha) \right] - \frac{K_y'(\Re\alpha)}{\beta_+} J_o(\beta_-^{1/2} \Re\alpha) \quad (53)$$

where,

$$Q_* = \frac{1}{I_o(\sigma_+^{1/2} \Re\alpha)} \left[ \gamma_1 \Theta_w + \frac{K_y(\Re\alpha)}{\sigma_+} J_o(\sigma_-^{1/2} \Re\alpha) \right]$$

$$K_y(r) = \left[ 1 - \left\{ \gamma \Re \varepsilon P e_h (K + K_1 x) + \gamma \Re \varepsilon \left( L_* I_o(\Omega_+^{1/2} r) - \frac{K_x(r)}{\Omega_+} J_o(\Omega_-^{1/2} r) + L_* I_o(\sigma_+^{1/2} r) - \frac{K_v(r)}{\sigma_+} J_o(\sigma_-^{1/2} r) + N_* I_o(\beta_+^{1/2} r) - \frac{K_w(r)}{\beta_+} J_o(\beta_-^{1/2} r) \right) \right\} \frac{\sigma_-^{1/2} r^2}{2} \right]$$

$$K_x(\Re\alpha) = \left[ 1 - \left\{ \gamma \Re^2 P e_h (K + K_1 x) + \Re \varepsilon \gamma \left( I_o(\Omega_+^{1/2} \Re\alpha) + \frac{K_x(\Re\alpha)}{\Omega_+} J_o(\sigma_-^{1/2} \Re\alpha) + L_* I_o(\sigma_+^{1/2} \Re\alpha) - \frac{K_v(\Re\alpha)}{\sigma_+} J_o(\sigma_-^{1/2} \Re\alpha) + N_* I_o(\beta_+^{1/2} \Re\alpha) - \frac{K_w(\Re\alpha)}{\beta_+} J_o(\beta_-^{1/2} \Re\alpha) \right) \right\} \frac{\sigma_-^{1/2} (\Re\alpha)^2}{2} \right] \quad (54)$$

$$K_x(\Re\alpha) = \left[ 1 - \left\{ \gamma \Re^2 (P e_h + P e_m) (K + K_1 x) + 2 \gamma \Re \varepsilon \left( L_* I_o(\sigma_+^{1/2} \Re\alpha) - \frac{K_v(\Re\alpha)}{\sigma_+} J_o(\sigma_-^{1/2} \Re\alpha) + N_* I_o(\beta_+^{1/2} \Re\alpha) - \frac{K_w(\Re\alpha)}{\beta_+} J_o(\beta_-^{1/2} \Re\alpha) \right) \right\} \frac{\sigma_-^{1/2} (\Re\alpha)^2}{2} \right]$$

$$K_v(\Re\alpha) = \frac{\sigma_-^{1/2} (\Re\alpha)^2}{2} \left\{ - \gamma \Re^2 P e_h K + \gamma \Re \varepsilon \left( 1 + \frac{\Omega_+ (\Re\alpha)^2}{4} \right) - \frac{\gamma \Re \varepsilon K_u (\Re\alpha)}{\Omega_+} \left( 1 - \frac{\Omega_- (\Re\alpha)^2}{4} \right) \right\}$$

$$K_w(\Re\alpha) = \frac{\beta_-^{1/2} (\Re\alpha)^2}{2} \left\{ - \gamma \Re^2 P e_h K + \gamma \Re \varepsilon \left( 1 + \frac{\Omega_+ (\Re\alpha)^2}{4} \right) - \frac{\gamma \Re \varepsilon K_u (\Re\alpha)}{\Omega_+} \left( 1 - \frac{\Omega_- (\Re\alpha)^2}{4} \right) \right\}$$

$$K_u(\Re\alpha) = 1 - \frac{\gamma \Re^2 K}{2} (P e_h + P e_m) \left( \Re\alpha + \frac{\Omega_- (\Re\alpha)^3}{4} \right)$$

$$S_* = \frac{1}{I_o(\beta_+^{1/2} \Re\alpha)} \left[ \gamma_2 \Theta_w + \frac{K_y(\Re\alpha)}{\beta_+} J_o(\beta_-^{1/2} \Re\alpha) \right]$$

$$T_* = \frac{1}{M_1^2 I_o (M_1 \mathfrak{R} \alpha x)} \left[ \mathfrak{R} K_1 x - Gr (Q_* I_o (\sigma_+^{1/2} \mathfrak{R} \alpha x) - \frac{K_y (\mathfrak{R} \alpha x)}{\sigma_+} J_o (\sigma_-^{1/2} \mathfrak{R} \alpha x)) - Gc (S_* I_o (\beta_+^{1/2} \mathfrak{R} \alpha x) - \frac{K_y (\mathfrak{R} \alpha x)}{\beta_+} J_o (\beta_-^{1/2} \mathfrak{R} \alpha x)) \right]$$

### 3 Results and Discussion

In sections 2 we formulated and solved for the problem of the biomechanics of bifurcating green plants when the environmental thermal gradient is constant with intent on investigating the effects of bifurcation angle and soil nature on the xylem flow. The analyses of results show that the variations in the bifurcation angle and magnetic field have significant effects on the flow structure. To this end, using Maple12 computational software for various values of angle of bifurcation  $\alpha$  and soil parameter  $M^2$ , which accounts for the effect of soil nature on the flow model. For realistic values of  $Pr = 0.71$ ,  $Re = 0.03$ ;  $\gamma_1 = 0.6$ ,  $\gamma_2 = 0.6$ ,  $\gamma = 0.7$ ,  $\Phi_w = 2.0$ ,  $\Theta_w = 2.0$ ,  $\mathfrak{R} = 0.8$ ,  $\delta_1^2 = 0.2$ ,  $N^2 = 0.2$ ,  $\chi^2 = 0.2$  and for varying values of  $\alpha = 5, 10, 15, 20$  and  $M^2 = 0.1, 0.5, 1.0, 10$ , we have the results shown in fig. 2 – fig.15. These figures show the profiles for the velocities, concentration, temperature, Sherwood and Nusselt numbers, and they indicate that the flow velocity, concentration and Sherwood number increase with the angle of bifurcation (see Figs.2, 3, 4, 5, 6), whereas the increase in the magnetic field force decreases the velocity, temperature and Nusselt number (see Figs.7, 8, 9, 10, 11, 12, 13) but increases the concentration (see Figs.14, 15).

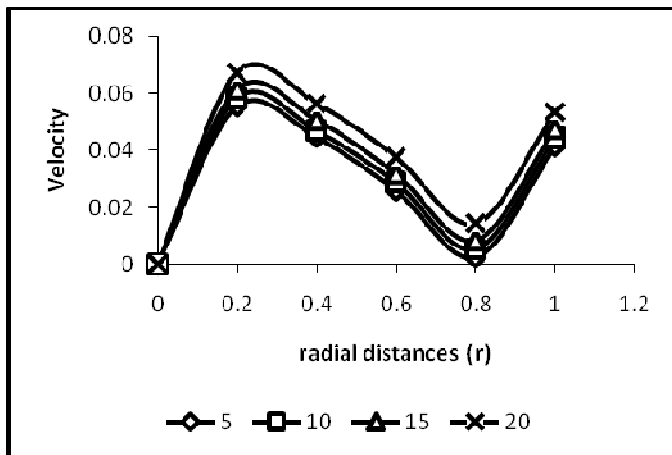


Fig. 2 Velocity –bifurcation angle ( $\alpha$ ) profiles at various radial distances ( $r$ ) in the daughter tube when  $Gr/Gc=0$

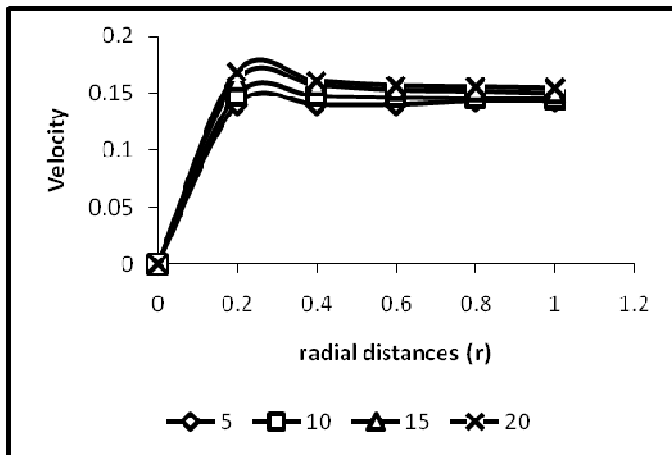


Fig. 3 Velocity-bifurcation angle ( $\alpha$ ) profiles at various radial distances ( $r$ ) in the daughter tube when  $Gr/Gc \neq 0$

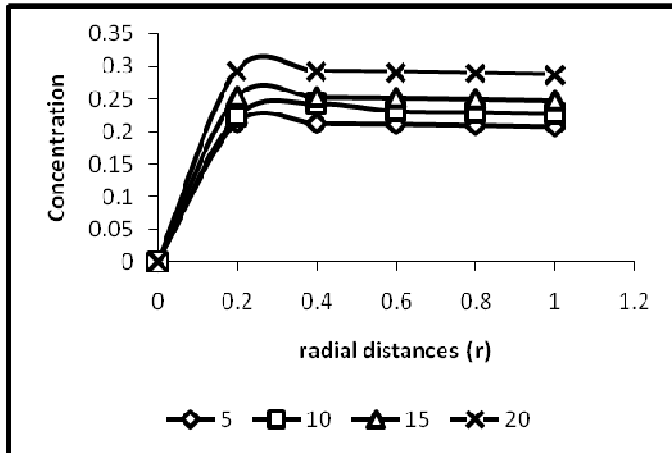


Fig. 4 Concentration –bifurcating angle ( $\alpha$ ) profiles at various radial distances (r) in the daughter tube when  $Gr/Gc=0$

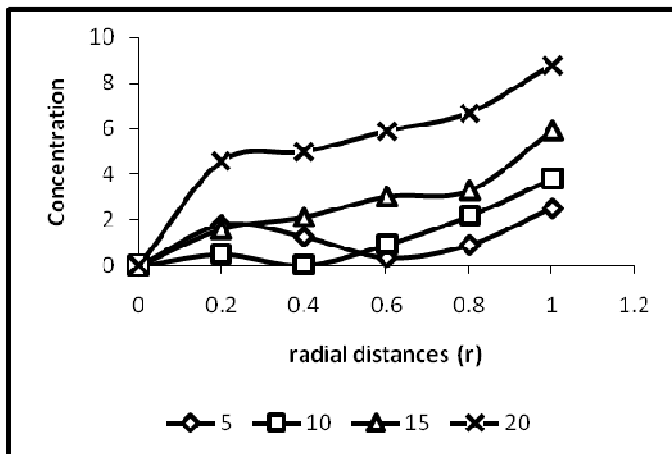


Fig. 5 Concentration-bifurcating angle ( $\alpha$ ) profiles at various radial distances (r) in the daughter tube when  $Gr/Gc \neq 0$

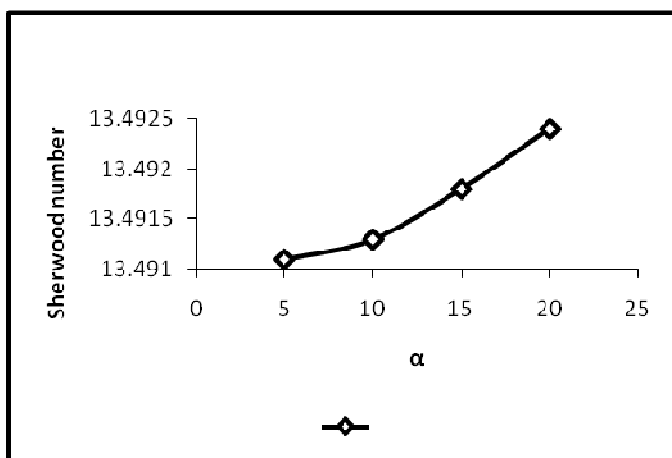


Fig.6 Sherwood number profiles for various bifurcating angles ( $\alpha$ ) in the daughter tube when  $Gr/Gc=0$

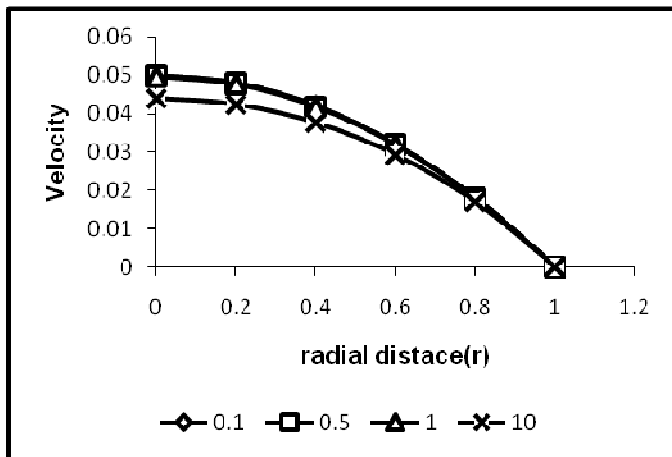


Fig 7 Velocity-magnetic field parameter ( $M^2$ ) profiles for various radial distances ( $r$ ) in the mother channel when  $Gr/Gc=0$

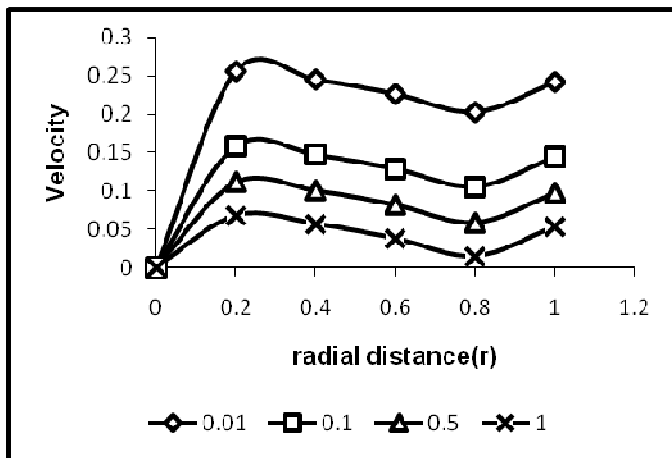


Fig. 8 Velocity-magnetic field parameter ( $M^2$ ) profiles for various radial distances in the daughter channel when  $Gr/Gc=0$

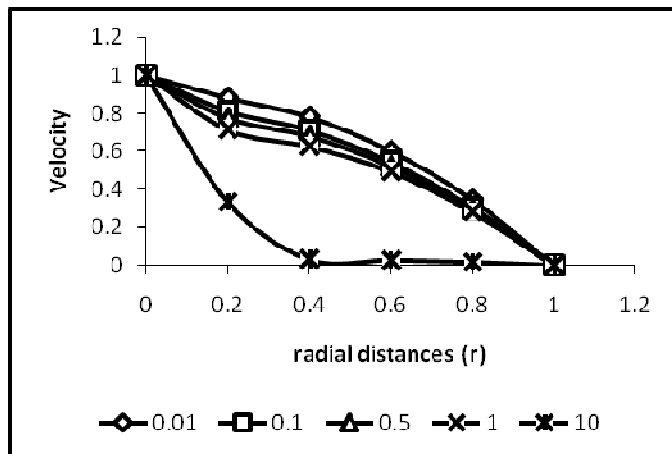


Fig. 9 Velocity- magnetic field parameter ( $M^2$ ) profiles at various radial distances ( $r$ ) in the mother tube when  $Gr/Gc \neq 0$



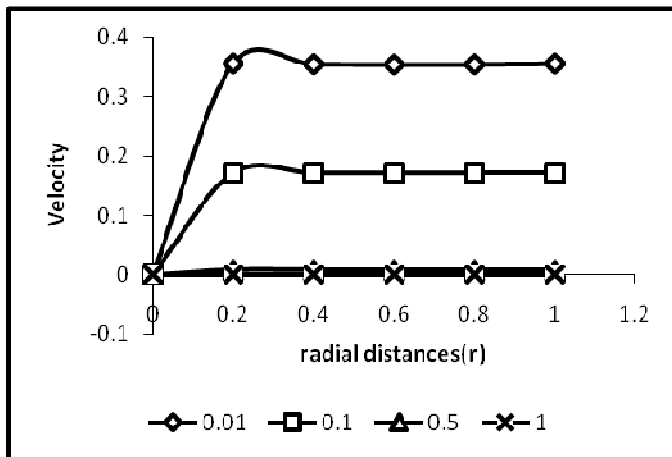


Fig. 10 Velocity- magnetic field parameter ( $M^2$ ) profiles at various radial distances (r) in the daughter tube when  $Gr/Gc \neq 0$

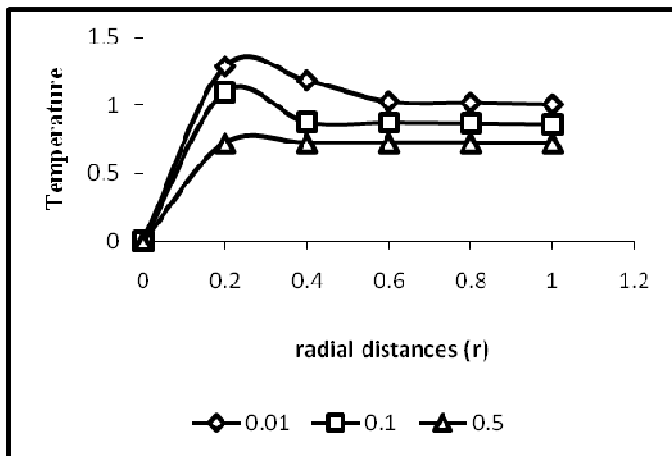


Fig.11 Temperature- magnetic field parameter ( $M^2$ ) profiles at various radial distances (r) in the daughter tube for  $Gr=0$

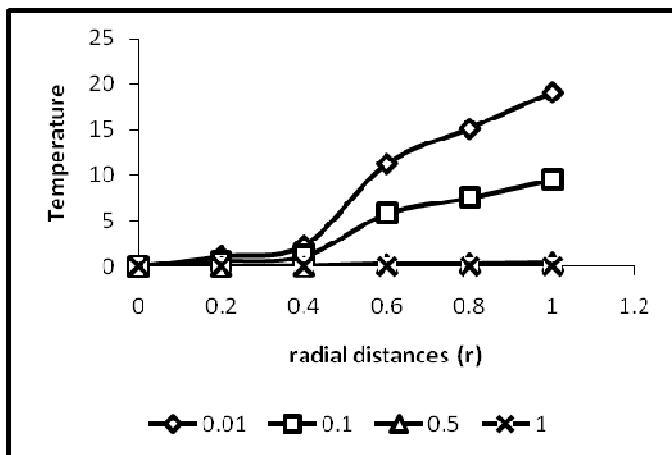


Fig. 12 Temperature- magnetic field parameter ( $M^2$ ) profiles at various radial distances (r) in the daughter tube for  $Gr \neq 0$

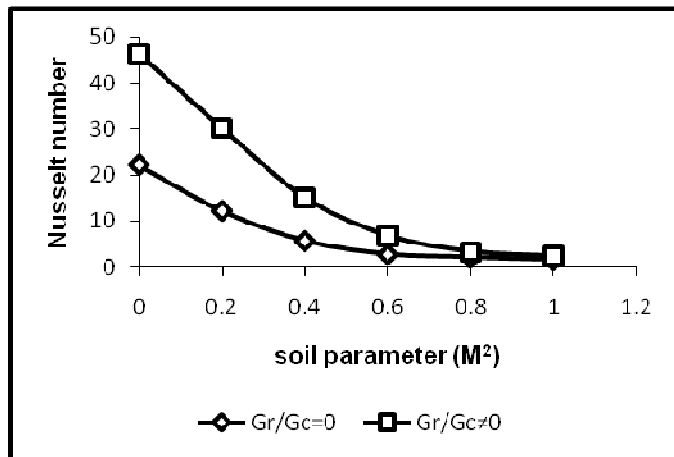


Fig. 13 Nusselt number profiles in the daughter channel for various soil parameter ( $M^2$ ) when  $Gr/Gc=0$  and  $Gr/Gc \neq 0$

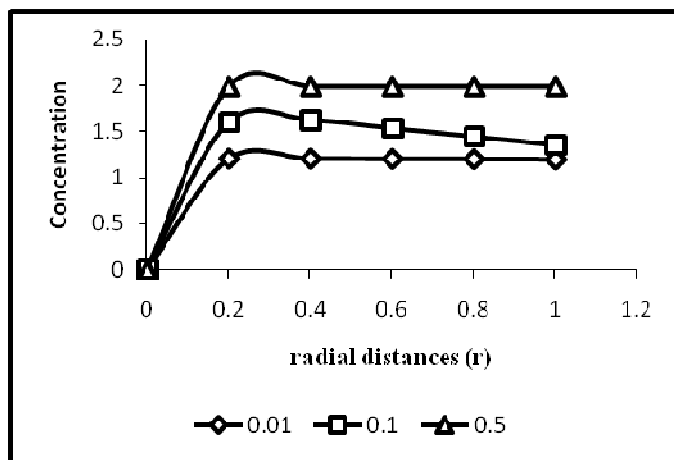


Fig. 14 Concentration-magnetic field parameter ( $M^2$ ) profiles at various radial distances ( $r$ ) in the daughter tube when  $Gr/Gc=0$

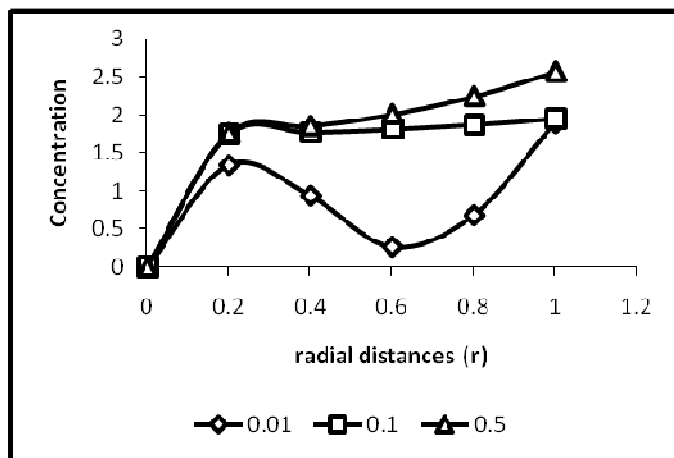


Fig. 15 Concentration- magnetic field parameter ( $M^2$ ) profiles at various values of radial distance ( $r$ ) in the daughter tube when  $Gr/Gc \neq 0$ .

The increase in the bifurcation angle narrows down the diameter of the daughter channel, resulting in an increase in the inlet pressure, which in turn increases the flow velocity. This accounts for what is seen in Fig.2

and Fig.3. These results are in good agreement with those of [9], [10], [12], [15] and [29]. More so, as the velocity increases, the rate and the quantity of soil mineral salt water transport are increased. This tends to explain the observation in Fig. 4 and Fig. 5.

Normally, there is an ambient or equilibrium concentration at the center of the channel where  $r=0$ . With the increase in the quantity of fluid, the concentration may exceed normal, such that the excess is transferred to the wall for a possible escape through diffusion. The rate of the transfer depends on the flow rate, which in turn depends on the angle of bifurcation and velocity, respectively, (see Fig. 6). The gradient in concentration helps to create favorable situation for convective or buoyancy force which increases the flow, too.

On the other hand, the chemical content of the soil mineral salt water is alkaline, and may contain some traces of acid. Therefore, the soil mineral salt water is electrolytic and exists as ions or charges. The motion of these charges in a magnetic field produces electric currents. The action of the magnetic field on the currents produces a mechanical force (the Lorentz force) which modifies the flow. In particular, the Lorentz force tends to freeze up the motion (see Fig. 7 – Fig.10). This is in consonance with the findings of [15], [20], [22], [23], [25] and [26].

More so, the decrease in the velocity due to the presence of magnetic field leads to a decrease in the kinetic energy of the fluid particles, and hence the temperature decreases. This accounts for what is noticed in Fig. 11 and Fig. 12. Additionally, the decrease in the temperature implies that the temperature of the system is low, and heat is not generated. For this, the rate heat transfer to the wall drops (see Fig. 13)

Furthermore, the soil mineral salt water is magnetically susceptible, therefore, is responsive to external magnetic field. Its material contents are fractionalized and polarized in the presence of magnetic field, and tend to flow toward the magnetic field and cluster around it. The magnetic force inhibits the fluid from flowing out of the field. This leads to a huge concentration of fluid in the field, and thus accounting for what is seen in Fig.14 and Fig.15.

The increase or decrease in the velocity, temperature and concentration factors has some tremendous attendant effects on the growth potential and productivity of the plant. For example, the increase in the velocity tends to increase the rate at which water and soil nutrients are made available to the plants. Other factors being constant, this enhances the growth and yield of the plant. On the converse, the reduction in the flow velocity adversely affects the growth and productivity of the plant. More so, the increase in the concentration or quantity of the fluid transported implies an increase in the plant nutrients absorbed in to the plant. Secondly, a high concentration of the fluid in the plant cells means that the fluid in the plant is at higher osmotic pressure than that in the soil such that more water and nutrients are forced into the plant. These processes help in the growth and yield of the plant.

Contrarily, the decrease in the temperature reduces the permeability of the plant cell membranes and makes the fluid more viscous, thus inhibiting the flow. This has adverse effects on the plant growth and yield. Similarly, it is seen that the Lorentz force which depends on the electrolytic strength of the mineral salt water tends to freeze up the flow velocity. Therefore, the variation in the electrolytic strength of the soil mineral salt water accounts for why some plants do well in some regions than in the others.

#### 4 Conclusion

The analysis of the results indicates that the velocity, concentration, Nusselt and Sherwood numbers increase with the bifurcation angle, whereas the magnetic field (or soil parameter) decreases the velocity and Nusselt number but increases the concentration and Sherwood number. These have tremendous agricultural implications. The increase in the velocity and concentration enhance the growth and yield of the plant. On the other hand, the variation in the electrolytic strength of the soil mineral salt water leading to lower or higher Lorentz force accounts for why some plants do well in some regions than in the others. Furthermore, in the absence of bifurcation angle (i.e.  $\alpha=0$ ) and the nature of the soil on which the plant grows the problem reduces to [4] model. Interestingly, the analysis presented in this model aids our understanding of the global biomechanics of green plants.

## References

- [1] Vines AE and Rees N. Plant and animal biology, vol.2, 4th ed. Pitman Books Ltd: London;1982
- [2] Ferraro VCA, Plumpton C. An introduction to magneto-fluid mechanics, 2nd ed. Clarendon Press: Oxford, U.K; 1966
- [3] Hughes WF and Brighton JA. Theory and problems of fluid dynamics. Schaum Publishing Company: New York; 1967.
- [4] Bestman AR. Global models for the biomechanics of green plants, Part 1. International Journal of Energy Research. 1991; 16:677– 684.
- [5] Rand RH. Fluid mechanics of green plant, Ann. Rev. Fluid Mechanics. 1983; 15:29-45.
- [6] Karl Niklas, Hanus-Christof Spatz, Julian Vincent. Plant biomechanics: an overview and Prospectus. American Journal of Botany. 2006; 93(10):1369-1378
- [7] Pedley TJ, Schroter RC, Sudlow M.F. The prediction of pressure drop and variation of resistance within the human bronchial airways. Resp. Physiology 1970; 9:387–405.
- [8] Liou TM, Chang TW, Chang WC. Effects of bifurcation angle on the steady flow structure in model saccular aneurysms. Experiments in Fluids. 1993; 289–295.
- [9] Smith FT, Jones MA. One-to-few and one-to-many branching tube flow. Journal of Fluid Mechanics. 2000: 423:1–32.
- [10] Smith FT, Jones MA. Modeling of multi–branching tube flows: large flow rates and dual solutions. IMA Journal of Mathematical Medical Biology. 2003; 20:183–204.
- [11] Smith FT, Ovenden NC, Frank P, Doorly DJ. What happens to pressure when a fluid enters a side branch. Journal of Fluid Mechanics. 2003; 479:231–58.
- [12] Pittaluga MB, Repetto R, Tubino M. Channel bifurcation in braided rivers: equilibrium configuration and stability, Water Resources Research. 2003; 39(3):1046 – 57.
- [13] Soulis. Journal of Biomechanics. 2004; 39:742–49.
- [14] Tadjar M, Smith FT. Direct simulation and modeling of basic 3-dimensional bifurcating tube flow. Journal of Fluid Mechanics. 2004; 519:1-32,
- [15] Okuyade WIA, Abbey TM. Analytic study of blood flow in bifurcating arteries, part 1- effects of bifurcating angle and magnetic field. International Organization of Scientific Research Journal of Mathematics. 2015. I.D: G54040 - (in press)
- [16] Rao VV, Ramana, Sobha VV. Heat transfer of a saturated porous flow in a rotating straight pipe. Proceeding of the Tenth National Heat and Mass Transfer Conference, Madurai Kamaraj University, Madurai. 1987; 13.
- [17] Avramenko AA, Kuznetsov AV. Flow in a curved porous channel with rectangular cross-section. Journal of Porous Media. 2008; 241-48. Doi: 10.1615/JporMedia.v.11.i3.20
- [18] Okuyade WIA, AbbeyTM. Analytic study of blood flow in bifurcating arteries, part 3- on wall shear stress. International Organization of Scientific Research Journal of Mathematics. 2015. I.D: G54041- (in press)
- [19] Shateyi S, Motsa SS, Sibanda P. Homotopy analysis of heat and mass transfer boundary

- layer flow through a non-porous channel with chemical reaction and heat generation. *The Canadian Journal of Chemical Engineering*. 2010; 88:975-982.
- [20] Kaur JP, Singh GD, Sharma RG. Unsteady porous channel flow of a conducting fluid with suspended particles. *Defence Science*. 1988; 38(1):13-20.
- [21] Abdel-Malek MB, HelalMM. Similarity solutions for magneto-force unsteady free convective laminar boundary-layer flow. *Journal of Computation in Applied Mathematics*. 2008;218:202–214.
- [22] Asadolah, Malekzadeh, Amir Heydarinasab, Bahram Dabir. Magnetic field effect on fluid flow characteristic in a pipe for laminar flow. *Journal of Mechanical Science and Technology*. 2011; 25:333-39.
- [23] Venkateswalu S, Suryanarayana Rao KV, Rambupal Reddy B. Finite difference analysis on convective heat transfer flow through porous medium in a vertical channel with magnetic field. *Indian Journal of Applied Mathematics and Mechanics*. 2011; 7(7):74–94.
- [24] Das S, Jana RN, Makinde OD. Mixed convection magneto-hydrodynamic flow in a channel filled with nano-fluids. *Elsevier Journal of Engineering Science and Technology*. 2015;244-255. DOI: <http://dx.doi.org/10.1016/j.jestch.2014.12.009>
- [25] Sharma PR, Kalpna Sharma, Tripti Mehta. Radiative and free convective effects on MHD flow through a porous medium with periodic wall temperature and heat generation or absorption. *International Journal of Mathematical Archive* 2014; 5(9):119-128
- [26] Okuyade WIA. MHD blood flow in bifurcating porous fine capillaries, *African Journal of Science Research*. 2015; 4(4):56-59.
- [27] Okuyade WIA, Abbey TM. Analytic study of blood flow in bifurcating arteries, part 2-effects of environmental temperature differentials, *International Organization of Scientific Research Journal of Mechanical Engineering*. 2015. I.D: G54083 - (in press)
- [28] Alphonsa Mathew, Singh KD. Span-wise fluctuating MHD convective heat and mass transfer flow through porous medium in a vertical channel with thermal radiation and chemical reaction. *International Journal of Heat and Technology*. 2015; 33(2). DOI:10.1820/Ijht.330222
- [29] Okuyade WIA, Abbey TM, Steady MHD fluid flow in a bifurcating rectangular porous channel. *Advances in Research (Sciencedomain International)*. 2016; 8(3):1-17. DOI:10.9734/AIR2016.26399.
- [30] Krishna MV, Basha SC. MHD free convection three dimensional flow through a porous medium between two vertical plates. *International Organization of Scientific Research Journal of Mathematics*. 2016; 88-105. DOI: 10.9790/5728-121288105.